SAJSET
ISSN: 2992-3581

Savannah Journal of Science and Engineering Technology
Volume: 03; Issue: 03; Pages: 152-159; 2025.
www.sajsetjournal.com.ng

DOI: xx.xxxx.x/sajset-03-2025-0015

SAJSET
ISSN: 2992-3581

Application of a unified power flow controller to improve power security in Nigeria's 330kV grid

[1]Musa, S. Y., [1]Haruna, J., [1]Visa M. I. and [1]John, Z.

[1]*Department of Electrical and Electronics Engineering, Modibbo Adama University Yola, Adamawa State, Nigeria*
saiduymusa@mau.edu.ng; jinkaiharuna@gmail.com; visaibrahim@gmail.com; support@zando.co.za

Paper History
Received: 01st March, 2025
Accepted: 26th April, 202
Published: May, 2025

Corresponding author
Visa, M. I.
visaibrahim@gmail.com

Abstract:

The study is motivated by the need to reduce transmission losses and improve voltage stability in Nigeria's national grid using advanced control technologies. This study explores the use of a Unified Power Flow Controller (UPFC) to enhance power security in Nigeria's national grid by reducing transmission line power losses. The UPFC is selected for its superior versatility among Flexible Alternating Current Transmission System (FACTS) devices. A voltage sensitivity index (VSI) method is employed to determine the optimal placement of the UPFC, while the bat algorithm optimization technique is utilized to identify its optimal size. Simulation results indicate a reduction in net active and reactive power losses from 106.58MW and 703.75MVAr to 84.23MW and 597.50MVAr, respectively. Additionally, voltage improvements were observed across most load buses, with a maximum enhancement of 0.1 pu recorded on three buses. The results imply that implementing an optimally placed and sized UPFC can significantly enhance the efficiency and stability of Nigeria's power grid by reducing transmission losses and improving voltage profiles. This study can be applied to improve the reliability and efficiency of power transmission systems in Nigeria and other developing countries facing similar grid challenges.

Keywords: *UPFC, FACTS, Voltage Sensitivity Index, Bat Optimization Algorithm.*

1. Introduction

The Nigerian national electrical power network continues to expand due to increasing power demand, leading to a system that is overstretched. The demand placed on the network exceeds its operational capacity, meaning that existing infrastructure is being fully utilized. When a power system operates at such a state, it is pushed close to its thermal and stability limits and frequently experiences contingencies. Key factors affecting system security include voltage deviations, system overload, and real power losses. To address these challenges and enhance overall system security, various solutions have been explored, one of which is the implementation of Flexible Alternating Current Transmission Systems (FACTS) devices. [1, 2]

The development of FACTS technology has been documented in [3], leading to the introduction of various FACTS controllers. These controllers are based on voltage and current source converters and include devices such as Static Var Compensators (SVCs), Static Synchronous Compensators (STATCOMs), Thyristor Controlled Series Compensators (TCSCs), Static Synchronous Series Compensators (SSSCs), and Unified Power Flow Controllers (UPFCs). Among these, the UPFC is the most advanced and efficient as it can regulate three critical transmission parameters: voltage magnitude, line impedance, and phase angle [3].

Over the past decade, several algorithms have been developed for the optimal integration of FACTS devices, particularly for UPFC placement within power networks. These include sensitivity-based approaches [5], evolutionary-programming-based load flow algorithms [6], genetic algorithms [7], particle swarm optimization [8], artificial neural networks (ANNs) [9, 10], and self-adaptive differential evolutionary (SADE) algorithms [11]. These methods have been used to determine the optimal placement and sizing of UPFCs within the power system.

There have been previous applications of UPFCs in improving the Nigerian power network. Research has explored UPFC placement methods [12, 13], its role in transient stability enhancement [14], real and reactive power control [15, 23], and voltage stability improvement [24].

This paper focuses on optimizing real power loss using the bat algorithm optimization technique. The Voltage Sensitivity Index (VSI) method is employed to identify the best location for UPFC installation in the Nigerian 330kV integrated power network [15]. A comparative analysis of network performance before and after UPFC installation is also presented.

2. Methodology

This study follows a structured approach consisting of the following steps: [16]

a. **Power Flow Analysis** – A Newton-Raphson-based power flow analysis is conducted on the study system to determine the initial (pre-compensation) bus voltages, the available power at each bus, and the power losses in different branches of the network.
b. **VSI Calculation** – The voltage sensitivity indices (VSIs) for all load buses are computed to identify the weakest bus, which serves as the optimal location for UPFC placement.
c. **Optimal UPFC Sizing** – The bat algorithm is applied to determine the optimal size of the UPFC.
d. **Performance Evaluation** – The effectiveness of the proposed approach is assessed on the Nigerian 31-bus transmission network

2.1 Power flow analysis (PFA)

Power flow analysis, extensively covered in various studies, is a technique used to assess the steady-state operational condition of an interconnected power system by utilizing known parameters at its buses. The primary goal of PFA is to determine the voltage magnitudes and phase angles at each bus. Once these values are obtained, the power flow across the system and the associated losses in transmission lines can be estimated. Essentially, power flow analysis involves solving complex, nonlinear power balance equations, as represented in equations 1 and 2 [17].

$$P_i = \sum_{i=1}^{N} |V_i||V_j||Y_{ij}| \cos(\delta_i - \delta_j - \theta_{ij}), j = 1, \dots, N \quad (1)$$

$$Q_i = \sum_{i=1}^{N} |V_i||V_j||Y_{ij}| \sin(\delta_i - \delta_j - \theta_{ij}), j = 1, \dots, N \quad (2)$$

PFA is implemented in the following procedure:

Step 1: Form the nodal admittance matrix (Y_{ij}) [17].

Step2: Initialization: Set one of the generator buses (*N*) as the slack bus with voltage magnitude $|V_N| = 1$ and angle δ_N =0.0. For the load buses, real power P_{isch} and reactive power *Q* is being specified. Voltage magnitudes and phase angles are initialized with the slack bus values. For the generator buses, V_i and P_i are specified and the phase angles are set equal to the slack bus value. Initialize iteration counter *k* [17].

Step 3: Calculate the real power P_{ical} and reactive power Q_{ical} using equations 1 and 2 respectively [17].

Step 4: Form the Jacobian Matrix J.

Step 5: Calculate the power differences ΔP_i and ΔQ_i for all the load buses using equations 3 and 4 [17].

$$\Delta P_i = P_{isch} - P_{ical}^{k} \quad (3)$$

$$\Delta Q_i = Q_{isch} - Q_{ical}^{k} \quad (4)$$

Step 6: Choose the tolerance values

Step 7: Stop the iteration if all ΔP_i and ΔQ_i are within the tolerance values.

Step 8: Update the values of V_i and δ_i using equations 5 and 6 respectively.

Step 9: Repeat from step 3 until all ΔP_i and ΔQ_i are within the tolerance values.

2.2 Computation of VSI

A bus that fails to sustain its load due to insufficient reactive power support is classified as a weak bus. The weakest bus is the most suitable location for installing a compensator. One of the most effective methods for identifying the weakest bus in a power system is by calculating stability indices. Various stability indices have been developed by researchers and documented in the literature [18 - 20]. Some of these indices include the Fast Voltage Stability Index (FVSI), Line Stability Index (Lmn), Voltage Collapse Prediction Index (VCPI), and Reactive Power Voltage Stability Index (RPVSI). Additional indices such as the Power Transfer Stability Index (PTSI), Line Voltage Stability Index (LVSI), and Equivalent Node Voltage Collapse Index (ENVCI) are also commonly used [18].

The voltage at a bus in a power system is primarily influenced by reactive power rather than active power, except in cases where the system is heavily loaded, making the impact of active power on bus voltage more significant [19]. Consequently, assessing bus voltage stability is best achieved by analyzing the variations in bus voltage concerning reactive power, as expressed in equation 5 [19]

$$VSI = \frac{\partial V_i}{\partial Q_j} \quad (5)$$

The VSI in (7) is the Reactive Power Voltage Sensitivity Index (RPVSI). The computation of the RPVSI is by considering the linearized form of the nonlinear power balance equations. The linearized form is given in equation (8) [19]

$$\begin{bmatrix} \Delta P \\ \Delta Q \end{bmatrix} = \begin{bmatrix} J_1 & J_2 \\ J_3 & J_4 \end{bmatrix} \begin{bmatrix} \Delta \delta \\ \Delta |V| \end{bmatrix} \quad (6)$$

Reactive power is primarily influenced by variations in voltage magnitude rather than changes in phase angle. Likewise, real power is minimally affected by changes in phase angle. Therefore, it is reasonable to approximate by setting J2 and J3 in equation (8) to zero, leading to the simplified form in equation 7 [19].

$$\frac{\Delta |V|}{\Delta Q} = J_{4ij}^{-1} \quad (7)$$

The RPVSI are computed as in equation 8 [19].

$$RPVS_i = diag\{J_{4ij}^{-1}\} \quad (8)$$

A positive RPVSI indicates stable operation. A lower sensitivity index signifies a more stable bus, whereas a higher sensitivity index suggests a weaker bus.

2.3 Bat algorithm

The Bat Algorithm is an optimization technique inspired by the echolocation behavior of bats. Bats use echolocation to navigate, locate prey, and differentiate between objects even in complete darkness [21]. This advanced ability has been adapted to solve various optimization problems. Echolocation functions like a natural sonar system, where bats emit short, high-frequency sound pulses, wait for the echoes to return after bouncing off

objects, and use this information to determine distance. This mechanism enables them to distinguish between obstacles and prey, allowing effective hunting even in total darkness.[21]

The Bat Algorithm employs frequency tuning, making it the first optimization method of its kind in computational intelligence. Each bat in the algorithm is represented by a velocity and a position at iteration *t* within a *d*-dimensional search space. The position corresponds to a potential solution to the problem being optimized. As the algorithm iterates, the best solution *x* found so far is updated and stored [21].

2.3.1 Key characteristics of the bat algorithm

The key characteristics of the bat algorithm are:

a. **Echolocation for Sensing and Differentiation** – Bats use echolocation to measure distances and can distinguish between prey and environmental obstacles [21].
b. **Adaptive Flight Behavior** – Bats move randomly with velocity (*vx*) at position (*xi*), adjusting their frequency (*f*), wavelength (*λ*), and loudness (*A0*) to search for prey. They can also modify their pulse emission rate ($r \in [0,1]$) depending on the proximity of the target [21].
c. **Loudness Adjustment** – The loudness of emitted pulses decreases from an initial value (*A0*) to a minimum threshold (*Amin*) as the search progresses [21].

2.3.2 Advantages of the Bat Algorithm:

The advantages of the bat algorithm are as follows

a. **Frequency Tuning** – Unlike other swarm intelligence methods such as PSO (Particle Swarm Optimization), SA (Simulated Annealing), and HS (Harmony Search), the Bat Algorithm utilizes frequency tuning to enhance the search process [22].
b. **Automatic Zooming** – BA can automatically focus on promising solution regions, leading to faster convergence in the early search stages compared to other metaheuristic algorithms [22].
c. **Dynamic Parameter Control** – Unlike many optimization methods that rely on fixed, pre-tuned parameters, BA allows dynamic adjustment of key parameters (*A* and *r*). This adaptability enables a smooth transition from exploration to exploitation as the optimal solution is approached [22].

In this study, the Bat Algorithm is utilized due to these advantages, particularly its efficiency in optimization tasks. As stated in Yang [21], the mathematical expressions for updating positions and velocities can be formulated as follows:

$$f_i = f_{min} + (f_{max} - f_{min}) \quad (9)$$

$$V_i^t = V_i^{t-1} + (X_i^t - X^*) f_i \quad (10)$$

$$X_i^t = X_i^{t-1} + V_i^t \quad (11)$$

Where $\beta \in [0,1]$ is a random vector drawn from a uniform distribution.

In this context, x_* represents the current global best position (solution) obtained by comparing all solutions among the *n* bats. A new solution for each bat is generated locally through a random walk, expressed as:

$$X_{new} = X_{old} + \varepsilon A \quad (12)$$

Furthermore, the loudness and pulse emission rates can be adjusted throughout the iterations. The equations used to modify the loudness and pulse emission rates are provided below.

$$A_i^{t-1} = \alpha A_i^i \quad (13)$$

$$r_i^{t-1} = r_i^o [1 - \exp(-yt)] \quad (14)$$

Where $0 < \alpha < 1$ and $\gamma > 0$ are constants. For any $0 < \alpha < 1$ and $y > 0$, we have:

$A_i^t \to 0$; $r_i^t \to r_i^0$ as $t \to \infty$The initial loudness A0 can typically be (1, 2), while the initial emission rate r_i^0 can be (0, 1).

2.4 Objective Function

This study aims to minimize real power losses to achieve maximum power transfer capability. Mathematically, the objective function can be expressed as in equation 15 and 16 [22]:

$$f = \min(P_{loss}) \quad (15)$$

$$P_{loss} = \sum_{i=1}^{Ntl} G_{ij} \left[V_i^2 + V_j^2 - 2V_i V_j \cos(\delta_i - \delta_j)\right] \quad (16)$$

Where G_{ij} represents the conductance of line ij, V_i and Vj are the voltage magnitudes at the sending and receiving ends of the line, respectively. δ_i and δ_j denote the phase angles of the end voltages. Nti is the total number of transmission lines.

The equality constraints are shown in equations 17 and 18 [22]:

$$P_{Gi} - P_{Di} - V_i \sum_{j=1}^{Nb} V_j (G_{ij} \cos(\delta_i - \delta_j) + B_{ij} \sin(\delta_i - \delta_j)) = 0 \quad (17)$$

$$Q_{gi} - Q_{Ci} - Q_{Di} - V_i \sum_{j=1}^{Nb} V_j (G_{ij} \sin(\delta_i - \delta_j) - B_{ij} \cos(\delta_i - \delta_j)) = 0 \quad (18)$$

Where P_{Gi} represents the real power generation at bus i, P_{Di} is the power demand at bus i, and Nb denotes the number of PQ nodes in the system.

Similarly, Q_{Gi} refers to the reactive power generation at bus i, Q_{Di} is the reactive power demand at bus i, and Q_{Ci} represents the reactive power from compensation nodes. According to Cui, *et al.* [22] the inequality constraints are:

Voltage Limits for Generator Buses is shown in equation 19 [22]

$$V_{Gi}^{min} \le V_{Gi} \le V_{Gi}^{max} \quad (19)$$

Where V_{Gi}^{min} is the minimum voltage at the generator bus, V_{Gi} represents the actual voltage at the generator bus, and V_{Gi}^{max} is the maximum voltage at the generator bus.

Real Power Generation Limits is shown in equation 20 [22].

$$P_{Gi}^{min} \leq P_{Gi} \leq P_{Gi}^{max} \quad (20)$$

Where P_{Gi}^{min} is the minimum real power at the generator bus, P_{Gi} denotes the actual real power at the generator bus, and P_{Gi}^{max} is the maximum real power at the generator bus.

Reactive Power Generation Limits is shown in equation 21 [22]:

$$Q_{Gi}^{min} \leq Q_{Gi} \leq Q_{Gi}^{max} \quad (21)$$

Where Q_{Gi}^{min} is the minimum reactive power at the generator bus, Q_{Gi} represents the actual reactive power at the generator bus, and Q_{Gi}^{max} is the maximum reactive power at the generator bus.

UPFC Limits is shown in equation 22:

$$V_{vr}^{min} \leq V_{vr} \leq V_{vr}^{max} \quad (22)$$

Where V_{vr}^{min} is the minimum shunt converter voltage magnitude (p.u), V_{vr} represents the actual shunt converter voltage magnitude (p.u), and V_{vr}^{max} is the maximum shunt converter voltage magnitude (p.u).

The series converter voltage inequality is shown in equation 23.

$$V_{cr}^{min} \leq V_{cr} \leq V_{cr}^{max} \quad (23)$$

Where V_{cr}^{min} represents the minimum series converter voltage magnitude (p.u), V_{cr} is the actual series converter voltage magnitude (p.u), and V_{cr}^{max} denotes the maximum series converter voltage magnitude (p.u).

2.5 Input parameters of the bat algorithm

The table 1 below presents the input data used for the Bat Algorithm.

Table 1: Input Parameters of Bat Algorithm

S/N	Parameters	Quantity
1	Number of iterations	50
2	Number of populations	20
3	Pulse rate	0.9
4	Loudness	0.9

2.6 Study system and data presentation

The transmission line data provides the impedance per unit length for each line segment, while the bus data includes details such as real power, reactive power, voltage magnitude, and phase angle at each bus. The network consists of 31 buses, nine of which are generator buses, while the remaining are load buses. The Egbin power station was selected as the slack bus due to its strategic location within the network and its highest generating capacity. The one-line diagram and additional details can be found in the appendix of this paper.

3. Results and discussion

3.1 Optimal Location of the UPFC

The calculated RPVSI values for the Nigerian 330kV network are presented in Table 2.

From Table 2, bus 19 has the highest RPVSI value, indicating that it is the weakest bus and the most suitable location for UPFC placement.

Table 2: VSI result for load buses

S/No	Load Bus Number	Voltage Sensitivity Index (VSI)	Bus Weakness Ranking
1	10	0.0253	9
2	11	0.0061	19
3	12	0.0073	17
4	13	0.0330	7
5	14	0.0601	4
6	15	0.0107	15
7	16	0.0062	18
8	17	0.2631	2
9	18	0.0150	12
10	**19**	**0.2878**	**1**
11	20	0.0074	16
12	21	0.0060	20
13	22	0.1514	3
14	23	0.0251	10
15	24	0.0141	14
16	25	0.0207	11
17	26	0.0041	21
18	27	0.0470	5
19	28	0.0032	22
20	29	0.0310	8
21	30	0.0150	13
22	31	0.0364	6

3.2 UPFC Size

The optimal UPFC size was determined using the Bat Algorithm, resulting in a value of 182.0438 MVAr.

3.3 Validation of the Technique

The power flow analysis was repeated using the Newton-Raphson method on the system with the appropriately sized and positioned UPFC, and the following results were obtained. The variations of line losses before and after installation of UPFC are given in Table 3. A graphical representation of the real power before and after UPFC placement (base case) is shown in Figure 1.

A graphical representation of the reactive power before and after the placement of the UPFC (base case) is shown in Figure 2. The voltage magnitudes of the buses in the 31-bus network, both before and after the installation of the UPFC, are presented in Table 4 and illustrated graphically in Figure 3.

Table 2 presents the calculated Relative RPVSI values for the load buses in the Nigerian 330 kV transmission network. These values help identify the buses most vulnerable to voltage instability under load variations. Among the evaluated buses, bus 19 exhibits the highest RPVSI value, signifying it as the weakest bus in terms of voltage stability. This makes it the most appropriate location for placing the Unified Power Flow Controller (UPFC), as installing the device at this point is expected to yield the most significant improvement in voltage support and overall system stability, while Table 3 provides a summary of the total line losses in the Nigerian 330 kV transmission network before and after the implementation of the Unified Power Flow Controller (UPFC). The data clearly show that the installation of the UPFC led to a substantial reduction in both real (active) and reactive power losses.

Table 3: Summary of Line Losses before and after UPFC Placement

S/N	Branch		Real Power Loss			Reactive Power Loss		
	From Bus	To Bus	MW Before UPFC	MW After UPFC	Diff. in MW	MVar Before UPFC	MVar After UPFC	Diff. in MVar
1	1	12	2.0974	1.9309	0.1665	16.3979	15.0963	1.3016
2	1	16	1.6586	1.5595	0.4991	12.5706	11.8194	0.7509
3	1	20	1.2386	1.1741	0.0645	9.3871	8.8982	0.4889
4	2	21	0.0843	0.0083	0.0760	0.6746	0.0663	0.6083
5	4	21	0.1084	0.0119	0.0965	0.8958	0.0984	0.7974
6	7	28	1.2143	1.2143	0.0000	103.0546	103.0546	0
7	7	27	1.3159	1.3167	-0.0008	14.7137	14.7233	-0.0096
8	8	29	7.2287	6.4932	0.7355	62.0818	55.7652	6.3166
9	8	30	0.1538	0.1521	0.0017	1.1659	1.1529	0.0130
10	8	18	0.6965	0.7259	-0.0294	5.2785	5.5018	-0.2233
11	9	24	0.9491	0.9069	0.00422	7.4200	7.0903	0.3297
12	10	27	0.5152	0.5640	-0.0488	43.8833	48.0400	-4.1567
13	10	11	0.2804	0.3882	-0.1078	2.4037	3.3285	-0.9248
14	10	12	0.7169	0.6062	0.1107	4.9888	4.2189	0.7699
15	11	24	0.1604	1.1536	-0.9932	9.2829	9.2286	0.0543
16	11	4	0.1888	0.5546	-0.3658	1.4577	4.2825	-2.8248
17	11	15	0.1268	0.1717	-0.0449	1.0768	1.4573	-0.3805
18	11	2	0.6474	0.3423	0.3051	5.5911	2.9566	2.6345
19	12	11	0.1594	0.1824	-0.0227	1.2611	1.4430	-0.1819
20	13	10	0.2874	0.2984	-0.0110	2.4465	2.5399	-0.0934
21	13	12	0.6069	0.5581	0.0488	5.1523	4.7385	0.4138
22	14	31	2.4236	0.6200	1.8036	20.5585	5.2596	15.2989
23	14	17	6.5538	0.5958	5.9580	55.8795	5.0796	50.7999
24	15	25	0.7644	0.2689	0.4955	6.5652	2.3093	4.2559
25	15	26	0.0646	0.1025	-0.0379	0.5528	0.8769	-0.3241
26	15	3	7.6060	5.1673	2.4387	5.9158	4.0190	1.8968
27	16	12	0.2841	0.2412	0.0429	2.4153	2.0501	0.3652
28	16	20	0.0818	0.0740	0.0078	0.6955	0.6288	0.0667
29	17	19	0.1042	0.3014	-0.1972	0.7594	2.1957	-1.4363
30	20	23	0.3287	0.3292	-0.0005	2.5700	2.5738	-0.0038
31	25	31	2.7085	1.0536	1.6549	20.5277	7.9849	12.5428
32	25	26	3.0825	1.8597	1.2228	23.3618	14.0943	9.2675
33	26	5	32.3898	25.3584	7.0313	25.1921	19.7232	5.4689
34	27	6	3.8950	3.6353	0.2597	2.8563	2.6659	0.1904
35	27	8	17.8066	17.5264	0.2802	151.8679	149.4777	2.3902
36	29	22	5.2090	6.2416	-1.0326	57.1080	68.4288	-11.3208
37	29	14	1.8393	0.5416	1.2977	15.7395	4.6344	11.1051
	TOTAL		**106.5771**	**84.2301**	**22.3470**	**703.7499**	**597.5021**	**106.2478**

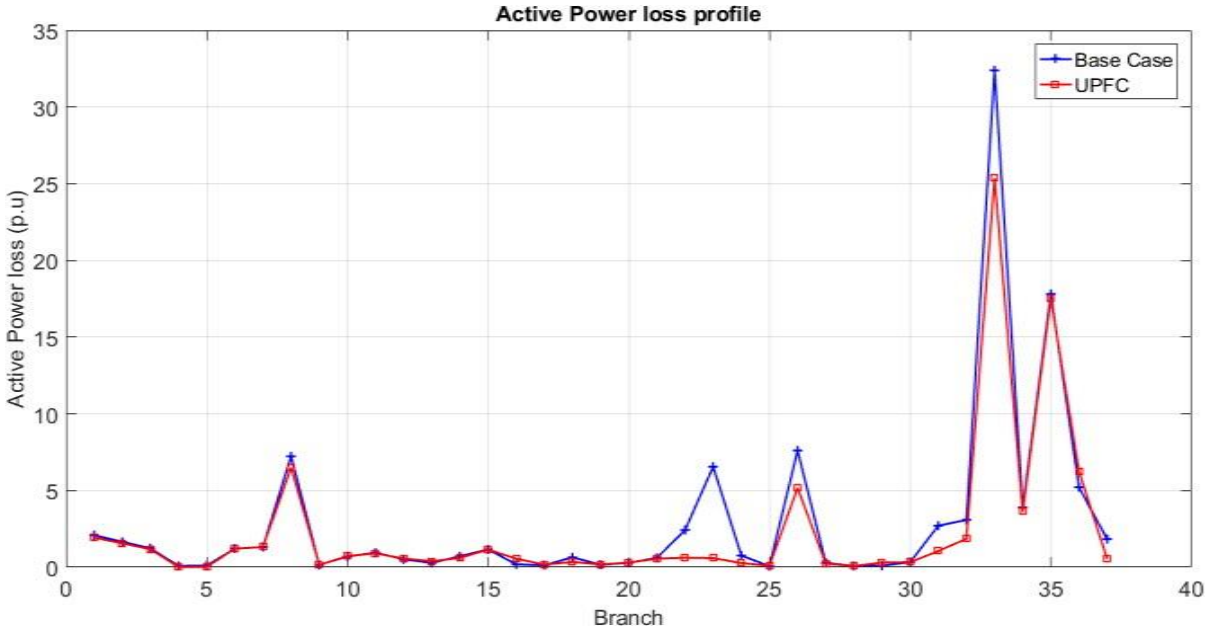

Figure 1: Variation of real Power Loss Profile

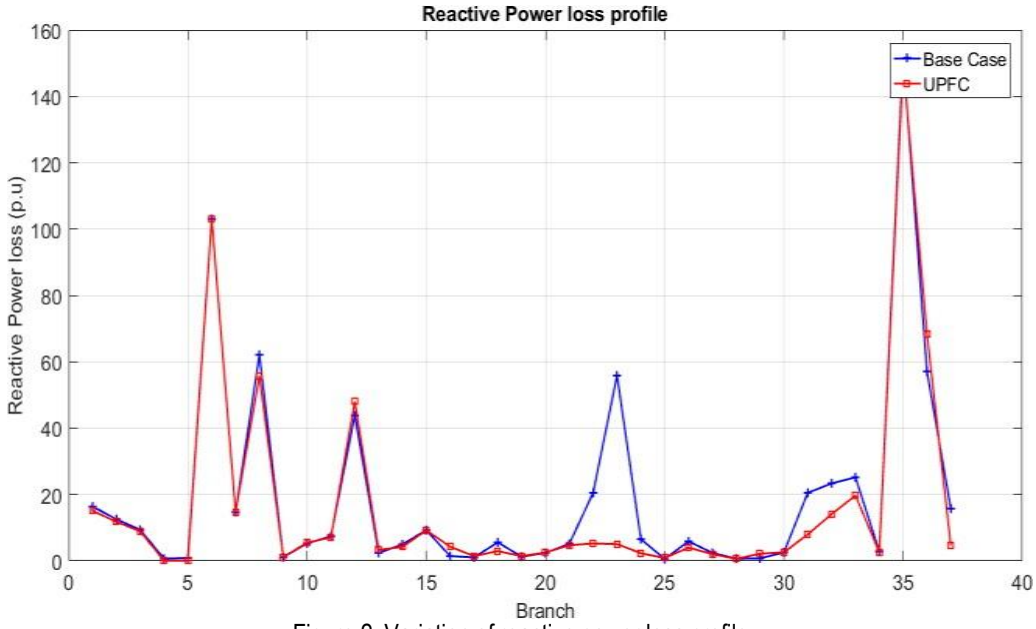

Figure 2: Variation of reactive power loss profile

Table 4: Voltage Profile Improvement

Bus No.	V(pu) Before UPFC	V(pu) After UPFC	V(pu) Improvement
1	1.0200	1.0200	0
2	1.0300	1.0300	0
3	1.0500	1.0500	0
4	1.0500	1.0500	0
5	1.0500	1.0500	0
6	1.0300	1.0300	0
7	1.0300	1.0300	0
8	1.0500	1.0500	0
9	1.0500	1.0500	0
10	1.0737	1.0748	0.0011
11	1.0616	1.0617	0.0001
12	1.0372	1.0374	0.0002
13	1.0557	1.0564	0.0007
14	1.1848	1.2848	0.1
15	1.0458	1.0458	0
16	1.0306	1.0308	0.0002
17	1.3836	1.4836	0.1
18	1.0451	1.0451	0
19	1.3942	1.4942	0.1
20	1.0303	1.0304	0.0001
21	1.0371	1.0371	0
22	1.0138	1.0143	0.0005
23	1.0217	1.0218	0.0001
24	1.0606	1.0606	0
25	1.0809	1.0875	0.0066
26	1.0384	1.0398	0.0014
27	1.0246	1.0246	0
28	0.7020	0.7020	0
29	1.0918	1.1823	0.0905
30	1.0569	1.0569	0
31	1.1237	1.1343	0.0106

Specifically, active power losses decreased from 106.58 MW to 84.23 MW, while reactive power losses dropped from 703.75 MVAr to 597.50 MVAr. This reduction indicates a more efficient transfer of electrical energy across the transmission lines, resulting in less energy dissipation and improved overall system performance. These results validate the effectiveness of the VSImethod and bat algorithm in determining the optimal location and size of the UPFC for maximum loss minimization.

Figure 1 illustrates the variation in real power loss across the transmission lines before and after the installation of the UPFC. The graph clearly shows a consistent reduction in real power losses across most lines, highlighting the UPFC's effectiveness in improving power flow and reducing energy dissipation. This reduction contributes to greater transmission efficiency and reliability. Similarly, Figure 2 presents the variation in reactive power loss before and after UPFC placement.

As with the real power losses, the reactive power losses also decreased significantly across the network. This improvement indicates enhanced voltage support and reactive power management, which are crucial for maintaining voltage stability and minimizing the risk of voltage collapse. Overall, both figures reinforce the conclusion that optimally deploying a UPFC improves the operational performance of the power grid.

Table 4 presents a comparison of the bus voltage magnitudes across the 31-bus Nigerian 330 kV transmission network before and after the installation of the UPFC. The data indicate a general improvement in voltage levels at most load buses, demonstrating the effectiveness of the UPFC in enhancing voltage stability. Notably, several buses that previously recorded voltages below the acceptable threshold showed significant recovery towards the nominal value of 1.0 pu.

The maximum voltage improvement observed was 0.1 pu at three buses, reflecting the UPFC's ability to mitigate voltage drops and support weak areas of the grid. Overall, the results confirm that optimal placement and sizing of the UPFC not only reduce power losses but also contribute to a more stable and reliable voltage profile across the network and Figure 3 shows the comparison of bus voltage magnitudes in the 31-bus Nigerian 330 kV network before and after the installation of the UPFC.

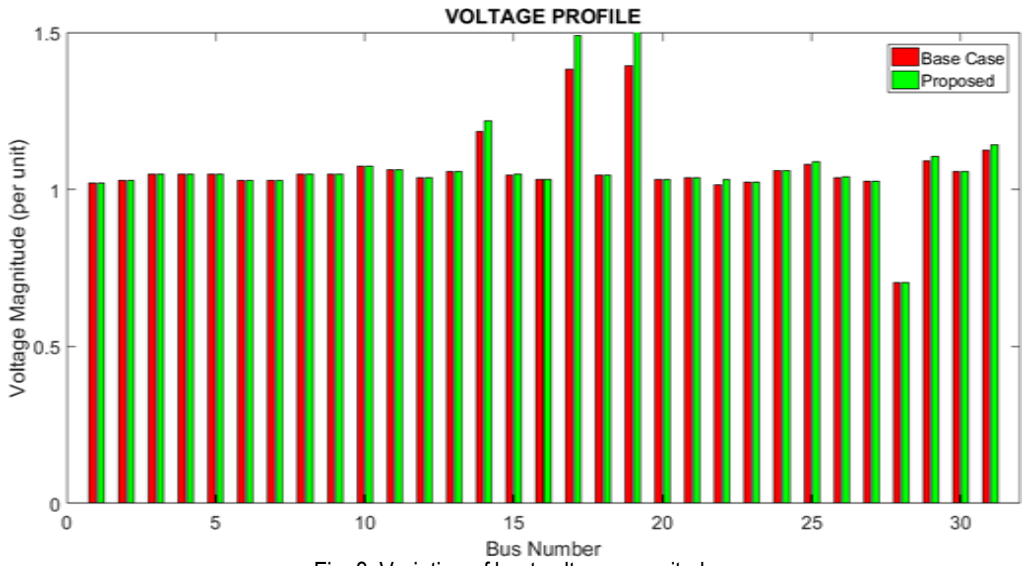

Fig. 3: Variation of bust voltage magnitude

The graph reveals a noticeable improvement in voltage levels across most buses following the UPFC deployment. Several buses that initially had voltages below the nominal value of 1.0 pu experienced significant enhancements, with the most considerable improvement being 0.1 pu on three buses. This upward shift in voltage profile demonstrates the UPFC's effectiveness in providing voltage support and stabilizing weak buses. The overall voltage enhancement contributes to a more balanced and stable power system, reducing the likelihood of voltage-related disturbances and improving power quality for end users.

4. Conclusions

The VSImethod was utilized to identify the weakest bus in the Nigerian 330kV, 31-bus network, determining the most suitable location for a compensator. The Bat Algorithm optimization technique was employed to ascertain the optimal size of the UPFC compensator. A simulation of the Nigerian 31-bus network incorporating the UPFC was conducted. The results revealed that bus 19 is the weakest, with the highest index value of 0.2878. The optimal UPFC size was determined to be 182.0438 MVAr. Additionally, the findings showed a significant reduction in real power loss, decreasing from 106.5771 MW in the base case (without UPFC) to 84.23 MW with UPFC. Reactive power loss also declined from 703.7499 MVAr to 597.5021 MVAr. Furthermore, voltage magnitudes across most buses in the network exhibited improvement.

References

[1]. Asibeluo U. N. and Madueme T. C., (2018) Risk-based security assessment of power system voltage drop: a case study of Nigerian 330kV 41-Bus transmission grid. *Nigerian Journal of Technology*, 37(3), 735 – 741.

[2]. Kumar, T. N. V. L. N. and Satya Narayana, R. V. S., (2018). Enhancing power system security: a multi-objective optimal approach to identify the location and size of SVC, *The IUP Journal of Electrical and Electronics Engineering*, 11(1), 45-58.

[3]. Hingorani, N. G., (1988). Power electronics in electrical utilities: role of power electronics in future power systems. *Proceedings of the IEEE on Future Power Systems*, 76(4), 481-482.

[4]. Nabavi-Niaki, A. and Iravani, M. R., (1996). Steady state and dynamic models of unified power flow controller (upfc) for power system studies, *IEEE Transactions on Power Systems*, 11(4), 19371943.

[5]. Singh, S. N. and Erlich, I., (2005). *Locating unified power flow controller for enhancing power system loadability*, International Conference on Future Power Systems. Amsterdam, Netherlands. pp. 1–5.

[6]. Wong, K. P., Yuryevich, J. and Li, A., (2003). *Evolutionary-programming-based load flow algorithm for systems containing unified power flow controllers*, IEE Proceedings-Generation, Transmission and Distribution. 150(4), 441–446.

[7]. Arabkhaburi, D., Kazemi, A., Yari, M., and Aghaei, J., (2006). *Optimal placement of UPFC in power systems using genetic algorithm*, In IEEE International Conference on Industrial Technology, Mumbai, India, pp. 1694–1699.

[8]. Saravanan, M., Slochanal, S. M. R., Venkatesh, P. and Abraham, J. P. S., (2007). Application of particle swarm optimization technique for optimal location of FACTS devices considering cost of installation and system loadability. *Electric Power System Research*, 77(3-4), 276–283.

[9]. Ghahremani, E. and Kamwa, I., (2012). *Maximizing Transmission Capacity through a Minimum Set of Distributed Multi-Type FACTS*, Proceedings of IEEE Power and Energy Society General Meeting, 27(4) San Diego, CA, USA, pp. 1-8.

[10]. Mohanty, A. and Viswavandya, M., (2015). *A novel ANN based UPFC for voltage stability and reactive power management in a remote hybrid system*, International Conference on Intelligent Computing, Communication and Convergence (ICCC-2014), Procedia Computer Science. 48, pp. 555 – 560.

[11]. Acharjee, P., (2016). Optimal power flow with UPFC

using security constrained self-adaptive differential evolutionary algorithm for restructured power system, *International Journal of Electrical Power and Energy Systems*, 76, 69–81.

[12]. Omorogiuwa, E. and Onohaebi, S. O., (2015). Optimal location of IPFC in Nigeria 330KV Integrated power network using GA Technique, *Journal of Electrical and Electronics*. 4(1). 1–10.

[13]. Nwohu, M. N., (2010). Optimal location of unified power flow controller (UPFC) in Nigerian Grid System, *International Journal of Electrical and Power Engineering*, 4(2), 147-153.

[14]. Bakare, G. A., Aliyu, U. O., Haruna, Y. S., and Abu, U. A. (2012). Transient enhancement of Nigerian Grid system using optimally tuned UPFC, Based on small population particle swarm optimization, *Asian journal of Natural and Applied Sciences*, 3(1), 79-90.

[15]. Musa, S. Y. and Haruna, J., (2020). Locating and sizing of unified power flow controller in power system network for power loss minimization using voltage sensitivity index and bat algorithm, *International Journal of Engineering Trends and Applications*, 7(2), 111-118

[16]. Naik, P., (2014). Power system contingency ranking using Newton Raphson load flow method and its prediction using soft computing techniques M.Tech. thesis, Dept. of Electrical Engineering., National Institute of Technology Rourkela, Rourkela, India,

[17]. Pruthviraja, L., Pradeepkumar, F. H., Ashok, M. and Mahesh Kumar, B. T., (2016). Load flow computation and power loss reduction using new particle swarm optimization technique, *International Journal of Scientific Development and Research*. 1(6), 114-117.

[18]. Bhadoriya, J. S. and Daheriya, C. K., (2014). An analysis of different methodology for evaluating voltage sensitivity, *International Journal of Advanced Research in Electrical, Electronics and Instrumentation Engineering,* 3(9), 12239-12246

[19]. Moradi, R. A., Davarani, R. Z. and Safarzaei, M., (2017). Performance evaluation of the voltage stability indices in the real conditions of power system, *American Journal of Energy and Power Engineering*, 4(5), 6-12

[20]. Amroune, M., Bourzami, A. and Bouktir, T., (2014). Weakest buses identification and ranking in large power transmission network by optimal location of reactive power supports, *TELKOMNIKA Indonesian Journal of Electrical Engineering*, 12(10), 7123 – 7130

[21]. Yang, X. S., (2010). A new metaheuristic bat - Inspired algorithm. Nature inspired Cooperative Strategies for Optimization Studies in Computational Intelligence, Springer International, Berlin. pp. 65-74.

[22]. Cui, X., Gao, J., Feng, Y., Zou, C. and Liu, H., (2018). Multi-objective reactive power optimization based on improved particle swarm algorithm, *IOP Conference Series: Earth and Environment al Science*, 108(5), 052081. DOI: 10.1088/1755-1315/108/5/052081

[23]. Mustapha, M., Musa, B. U. and Bakura, M. U. M., (2015). Modeling of unified power flow controller for the control of real and reactive power flow on 500KV interconnected system. University of Maiduguri, Faculty of Engineering Seminar Series. Vol.6, pp. 98-105.

[24]. Adeniji, O. A. and Mbamaliukem, P. O., (2017). Voltage stability enhancement and efficiency improvement of Nigerian Transmission system using UPFC, *American journal of Engineering research (AJER)*, 6(1), 37-43.